



Adsorption mechanism of sodium oleate and styryl phosphonic acid on rutile and amphibole surfaces

Wei XIAO^{1,2}, Ya-xin REN¹, Juan YANG¹, Pan CAO², Jun WANG², Wen-qing QIN², Guan-zhou QIU²

1. School of Resources Engineering, Xi'an University of Architecture and Technology, Xi'an 710055, China;

2. School of Minerals Processing and Bioengineering, Central South University, Changsha 410083, China

Received 6 November 2018; accepted 19 April 2019

Abstract: A reagent combination of sodium oleate (NaOl) and salicyl hydroxamic acid was employed as the roughing and scavenging collectors, whereas styryl phosphoric acid (SPA) and octanol were employed as the cleaning collectors. Results of bench-scale flotation demonstrate that the dosage of SPA can be reduced by about 80%, and that a better flotation index can be obtained using the proposed reagent system. The results of adsorption amount and contact angle measurements indicate that the rutile surface adsorbed not only a large amount of residual NaOl but also SPA and a small amount of NaOl remained on the amphibole surface in strong acidic solution. The hydrophobic difference between rutile and amphibole surfaces was therefore amplified in cleaning, and their further separation became much easier consequently.

Key words: rutile; amphibole; flotation separation; combined collector; synergistic adsorption mechanism

1 Introduction

Titanium and its alloys are extensively used in aviation, aerospace, marine, chemical, and pharmaceutical applications owing to their characteristics of small lightweights, high strengths, corrosion resistances, and magnetic resistances [1–5].

Rutile (TiO₂) and ilmenite (FeTiO₃) are mainly used as the raw materials in industrial extraction of titanium and its oxides [6,7]. The ilmenite resource in China corresponds to ~30% of all globally available resource. However, owing to the poor resource endowment, it has been considered to be non-exploitable. Therefore, high-grade titanium used in the defense industry and vast quantities of high-grade titanium dioxide are derived from rutile [8].

The quality of the concentrate is determined by the cost and technical difficulty in the smelting and further processing. Therefore, it is enriched and substantially purified in the separation process of raw ores [9,10]. However, the concentration and purification for primary rutile ore are challenging, owing to the mineralogy complexity, fine grain sizes of the gangues, and brittleness [11]. Despite the feasibility to obtain

concentrated rutile by combining gravity, magnetic, and electrostatic separation techniques, flotation is still one of the most efficient methods to enrich fine and ultra-fine primary rutile [12,13].

The efficiency of the flotation separation is directly affected by the adaptability of the reagent system. There are three types of collectors for primary rutile flotation: (1) fatty acid [14–16], (2) arsenic and hydroxamic acid [12,13], and (3) phosphonic acid [8] collectors. These reagents in rutile flotation are used independently or in simple combinations. However, the advantages and disadvantages of the coexistence of these reagents have not been yet fully investigated. For example, both sodium oleate (NaOl) and salicyl hydroxamic acid (SHA), which are inexpensive, can capture primary rutile at pH of 5–9, but with a relatively low selectivity [13,17]. Styryl phosphoric acid (SPA) has a high selectivity for primary rutile at acid conditions; however, it is expensive [8,18].

In this study, we reported a novel reagent system for flotation of primary rutile with a high efficiency at a low cost. In this reagent system, a reagent combination of NaOl and SHA was employed as the roughing and scavenging collectors, while SPA and octanol (OCT) were employed as the cleaning collectors. The pH values

for roughing and cleaning are in the ranges of 5 to 7 and 2 to 3, respectively. The combined reagent system overcomes the issues emerging not only from the inability of the TiO₂ grade to meet the requirement in the cleaning process owing to the low selectivity of sodium oleate but also from the expensive production owing to the large amount of SPA [19]. The results of adsorption amount and contact angle measurements revealed that the difference in surface hydrophobicity between rutile and amphibole was enhanced in the cleaning.

2 Experimental

2.1 Materials

Raw rutile samples used in the flotation tests were obtained from the Zaoyang mine in Hubei, China. The raw samples from a crushing and roller-crushing mill were stored at a fraction size of 3 mm, which were then ground to 74 μm (91%). After splitting, an analysis of the sample was performed to investigate principal chemical components and phases, and the results are presented in Tables 1 and 2, respectively. Table 1 shows that the grade of TiO₂ is only 3.08%; the primary impurity compounds are SiO₂, Al₂O₃, Fe₂O₃, CaO, and MgO. Table 2 indicates that the Ti-containing mineral is rutile, which is the only valuable mineral for further processing of the sample.

Table 1 Chemical components of rutile sample (%)

TTiO ₂	S	P	Fe ₂ O ₃	CaO
3.08	0.013	0.074	13.55	7.32
MgO	Al ₂ O ₃	SiO ₂	Na ₂ O	K ₂ O
6.95	16.72	43.28	2.38	0.22

Table 2 Phase composition and content of rutile sample (%)

Rutile	Ilmenite	Sphene	Amphibole	Andradite	Paragonite
2.43	0.63	0.04	67.33	11.76	7.74
Epidote	Chlorite	Quartz	Feldspar	Clay	Others
3.10	1.55	0.89	2.29	1.25	0.99

NaOl, SHA, SPA, and OCT were used as the collectors. Sodium silico fluoride (SSF) and sodium hexametaphosphate (SHMP) were used as the depressants. Sulfuric acid (H₂SO₄) and sodium carbonate (Na₂CO₃) were used as the pH modifiers. In addition, lead nitrate (Pb(NO₃)₂) and bismuth nitrate (Bi(NO₃)₃) were used as the activators. All reagents in this study were of analytical purity grade.

2.2 Methods

2.2.1 Micro-flotation tests

Micro-flotation tests were performed in an

inflatable hanging slot flotation apparatus (XFGC II) with an impeller rotation speed of 1800 r/min. The 2.0 g rutile samples were added to the flotation cell with 40 mL deionized distilled water. After conditioning for 1 min, the pH value of the slurry was adjusted using H₂SO₄ or NaOH. The collector was then added to the slurry, and conditioning was performed for 5 min. Subsequently, the pH of the slurry was adjusted to the appropriate value, followed by flotation performed for 3 min. The concentrates and tailings were collected, filtered, dried, and analyzed to evaluate the mass recovery of rutile.

2.2.2 Absorption amount measurements

The residual concentration of the collector in the solution after the adsorption was analyzed using a total organic carbon (TOC) analyzer (Shimadzu Corporation, Japan). Calibration curves were obtained for the relationship of NaOl (or SPA) and TOC contents in the solution. The collector concentration in the solution was obtained according to the TOC content. The adsorption amount was then calculated by

$$Q_e = \frac{V(C_o - C_e)}{m}$$

where Q_e is the collector amount adsorbed on the rutile surface (mol/g), C_o is the initial concentration of the collector (mol/L), C_e is the residual concentration of the collector in the solution (mol/L), V is the volume (L), and m is the mass of rutile (g).

2.2.3 Contact angle measurements

The contact angles of the rutile and amphibole surfaces before and after the treatment by the collectors were measured using the sessile drop method. Mineral samples were immersed in a collector solution for 10 min in different pH environments. The samples were then washed with distilled water with the same pH and dried in a vacuum oven. The measurements were performed using a JC200A Contact Angle Goniometer (Shanghai Powereach Digital Technology Equipment Co., Ltd., China). Images of water at the gas–solid–liquid interface were recorded using a high-speed amplifier camera. The contact angles were obtained by averaging four repeated measurements; the standard deviations were also calculated.

2.2.4 Bench-scale flotation

Bench-scale flotation experiments were performed in a 1.5 L XFD flotation cell. Ore samples (500 g) were added to a ball mill with a solid amount of 60%. After grinding and desliming, the samples (91% of their particle sizes were smaller than 74 μm) were placed in the flotation cell, in which the amount of solid minerals was 40%. The slurry solution was stirred for 3 min, followed by pH adjustment. The activator, depressant, collector, and frother were then added to the slurry in a

proper sequence, and the flotation was finally implemented. Both concentrates and tailings were filtered, dried, weighted, and sampled, and the recovery and grade of TiO_2 were calculated. The closed-circuit flowsheets of the rutile sample flotation are shown in Fig. 1. There is no difference between Figs. 1(a, b), except for the types of collectors. In Fig. 1(c), $\text{Bi}(\text{NO}_3)_3$ was used as the activator, and the pH of the slurry was adjusted in the range of 2–3 using H_2SO_4 , based on our previous study [8].

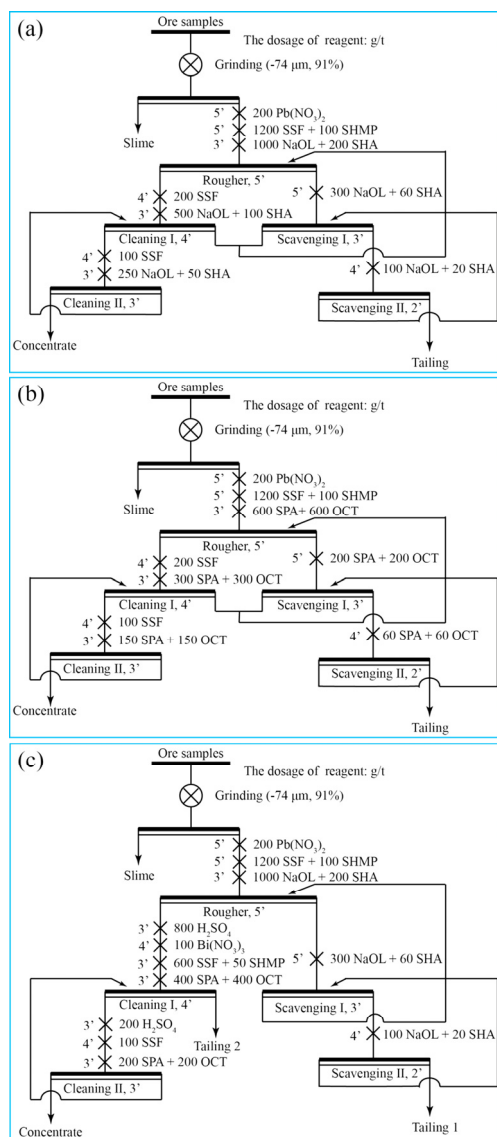


Fig. 1 Closed-circuit flowsheets of rutile sample flotation with NaOl and SHA (a), SPA and OCT (b), and NaOl and SHA (c) collectors of roughing and scavenging, and SPA and OCT as collectors in cleaning

3 Results

3.1 Micro-flotation test

In order to provide the optimal flotation condition of NaOl and SHA as the combined collectors,

micro-flotation tests of rutile were performed under various NaOl dosages, pH, and SHA dosages. The results are shown in Fig. 2. Figure 2(a) shows the effects of the concentration of a single NaOl collector on the rutile flotation. With the increase in the NaOl concentration from 600 to 1400 g/t, the flotation recovery was expected to stabilize after the rapid increase; the maximum value (approximately 84.62%) was observed at a NaOl concentration of 1200 g/t. However, the concentrate

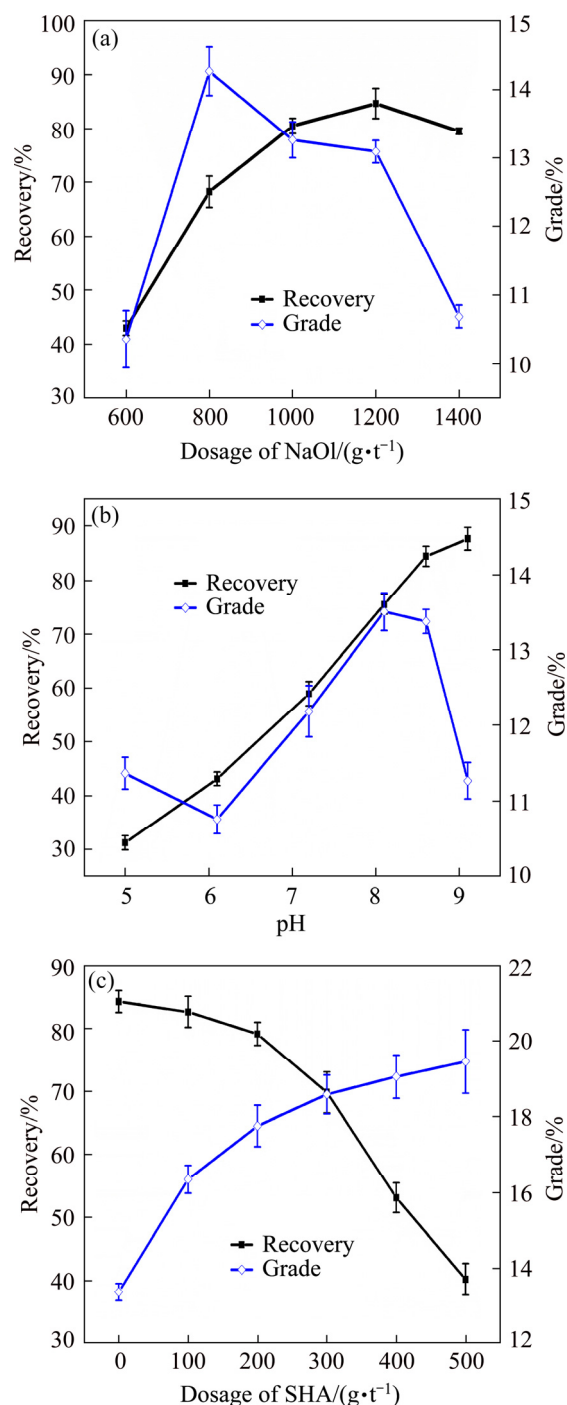


Fig. 2 Recovery and grade of rutile concentrate as function of dosage of NaOl (pH=8.5) (a), pH (dosage of NaOl: 1200 g/t) (b), and dosage of SHA (pH=8.5) (c), with fixed total collector dosage of 1200 g/t

grade rapidly increased and then gradually decreased; the maximum value was observed for a NaOl concentration of 800 g/t. We decided to obtain an improvement in the recovery rate in the roughing stage at the cost of a reduced grade. Therefore, a NaOl concentration of 1200 g/t was selected as the experimental dosage consumption and used in subsequent experiments.

In order to investigate the effect of the pH value on the rutile flotation when the NaOl dosage was 1200 g/t, micro-flotation tests of rutile were performed as a function of the pH value. As shown in Fig. 2(b), the recovery of rutile increases with the pH value in the range of 5–9, which suggests that the absorption of NaOl onto rutile also increases with pH. The rutile grade in the concentrate is relatively high when the pH is in the range of 7.5–8.5. When the pH exceeded 8.5, the grade rapidly decreased. Therefore, the pH value of 8.5 of the slurry was selected as the optimal pH for subsequent experiments.

Further, SHA was reported to increase the selectivity of the flotation system and improve the grade of the concentrate [20]. Micro-flotation tests were performed to investigate the effects of SHA on the NaOl flotation system. The dosage of the mixture collectors (NaOl and SHA) was fixed to 1200 g/t, and the pH of the slurry was adjusted to 8.5 (Fig. 2(c)). With the increase in the SHA concentration, the recovery of rutile in the concentrate slowly decreased; the recovery rapidly decreased when the SHA concentration exceeded 200 g/t. However, the change in the rutile grade in the concentrate exhibited the opposite trend; initially, it rapidly increased, followed by a gradual decrease when the SHA concentration exceeded 200 g/t. The SHA concentration of 200 g/t was selected as the optimal dosage, and the ratio of NaOl to SHA was 5:1.

The flotation optimization of the collector combination of SPA and OCT was performed similarly as the above optimization process; the dosage of SPA, pH, and dosage of OCT were selected as parameters in the optimization. The results are shown in Fig. 3. Figure 3(a) shows the effects of the SPA dosage on the rutile flotation at pH of 4.5. With the increase in the SPA dosage from 600 to 1600 g/t, the flotation recovery gradually increases. When the SPA dosage reaches 1200 g/t, the flotation recovery tends to be stable. The concentrate grade initially increased, and then slowly decreased, with a maximum value at a SPA dosage of 1200 g/t. Therefore, the SPA dosage of 1200 g/t was selected as the experimental dosage consumption and used in subsequent experiments.

Figure 3(b) shows the effects of pH on the rutile flotation using SPA (1200 g/t) as the collector. The recovery and grade of the rutile concentrate decrease with the increase in the pH value in the range of 4.5–7.0,

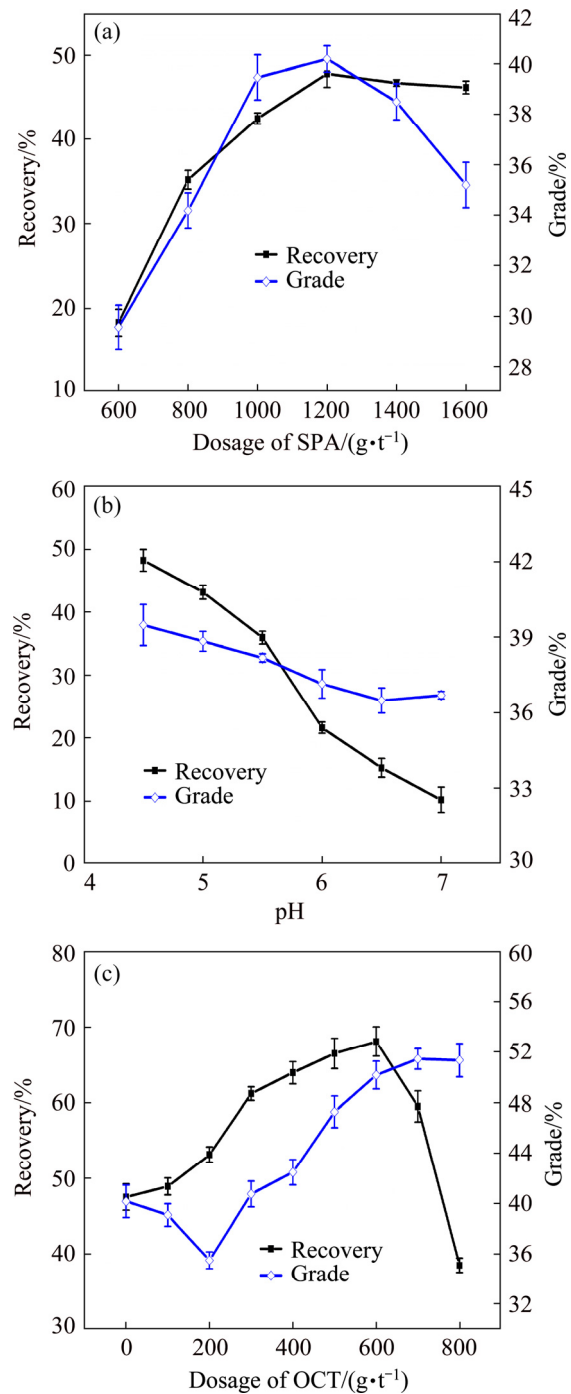


Fig. 3 Recovery and grade of rutile concentrate as function of SPA dosage (pH=4.5) (a), pH (dosage of SPA: 1200 g/t) (b), and OCT dosage (pH=4.5) (c), with fixed total collector dosage of 1200 g/t

which suggests that the absorption of SPA onto rutile decreases with the increase in the pH value. This was consistent with our previous results [8,21,22]. The pH value of the slurry was selected to be 4.5, as the optimal pH, which was used in subsequent experiments.

Higher alcohols were reported to increase the selectivity of a flotation system and improve the grade of

the concentrate [18]. Micro-flotation tests of rutile were performed as a function of the OCT dosage to investigate the effects of OCT on the SPA flotation system. The dosage of the mixture collectors (SPA and OCT) was fixed to 1200 g/t, while the pH value of the slurry was adjusted to 4.5. As shown in Fig. 3(c), with the increase in the OCT dosage, the recovery of rutile in the concentrate initially increased, followed by a rapid decrease when the dosage exceeded 600 g/t. However, the rutile grade in the concentrate was initially slightly lower and then steadily increased. The OCT concentration was selected to be 600 g/t as the optimal dosage, with a ratio of SPA to OCT of 1:1.

3.2 Bench-scale flotation measurements

In the above experiments, the flotation conditions and behaviors of the two combined collectors were different. The collector combination of NaOl and SHA was suitable for the weak alkaline flotation environment with almost no collection ability under acidic conditions. In contrast, the combination of SPA and OCT provided the opposite flotation recovery under the same pH conditions. In the flotation system of NaOl and SHA, the flotation recovery of rutile in the flotation concentrate was relatively high (approximately 80%), while the grade was low (only 18%). The combination of NaOl and SHA might be suitable for rough selection. In the flotation system of SPA and OCT, the flotation grade of rutile in the flotation concentrate was relatively high (approximate 50%), while the recovery was relatively low (only 67.45%). As SPA is expensive, the combination of SPA and OCT might be more suitable for re-purification of the coarse concentrate.

In order to compare the separation effects of the combined collectors (NaOl and SHA; SPA and OCT) for the primary rutile mine, we designed two closed-circuit experiments. The combination of NaOl and SHA was used as the collectors for roughing and scavenging, while the combination of SPA and OCT was used in the cleaning. The experimental flowcharts are shown in Fig. 1. The results of the bench-scale flotation in the different reagent systems are presented in Table 3. The recovery of Flow A utilizing NaOl and SHA as the collectors reached 87.01%, which indicated that NaOl and SHA had the highest ability to capture rutile. The loss of tailing from scavenging II was (12±0.7)%, which showed that the loss remained the same within the error range. For cost reduction, cheaper collectors were needed for roughing and scavenging. In Flow B, the grade of TiO₂ reached 68.22%, while the recovery was ~85.91%, showing that both SPA and OCT had high selectivities and collection abilities with respect to rutile. Further, a comparison was performed between Flow A and Flow B. The grade of TiO₂ in the concentrate of Flow B was

68.22%, which was considerably higher than the grade of 38.68% in Flow A, with insignificant changes in grade and recovery of gangue minerals. This suggested that SPA and OCT were advantageous in the cleaning than the combination of NaOl and SHA.

Table 3 Results of closed-circuit flowsheets

Flow	Product	Rate/%	Grade/%	Recovery/%
A	Concentration	7.40	38.68	87.01
	Tailing	90.60	0.43	11.84
	Slime	2.01	1.89	1.15
	Feed	100.00	3.29	100.00
B	Concentration	4.03	68.22	85.91
	Tailing	93.67	0.44	12.78
	Slime	2.31	1.83	1.31
	Feed	100.00	3.20	100.00
C	Concentration	3.51	78.68	83.43
	Tailing 1	89.76	0.42	11.39
	Tailing 2	4.63	2.89	4.04
	Slime	2.01	1.89	1.15
	Feed	100.00	3.31	100.00

By utilizing the advantages of Flow A and Flow B, Flow C was created. The roughing and scavenging stages were the same as those of Flow A, but the cleaning was different from that of Flow B. In Flow C, Bi(NO₃)₃ was used as the activator, and the pH was adjusted in the range of 2–3, according to the previous results [8]. The grade of TiO₂ in Flow C reached the optimal value (78.68%), more than 10% higher than that in Flow B, while the recovery was reduced by only 2.5%. Compared with Flows A and B, there were obvious advantages with respect to the flotation index. Furthermore, the dosage of SPA utilized in Flow C was only 45.8% of that of Flow B, which significantly reduced the cost of reagents.

3.3 Adsorption amount measurement

In order to reveal the origin of the differences in the rutile concentrate grade and recovery under different pH conditions, we measured the adsorption amounts of NaOl and SPA on the rutile and amphibole surfaces under different pH conditions. The results are shown in Figs. 4 and 5, respectively.

Figure 4 shows the adsorption amounts of SPA and NaOl on the rutile surface as a function of the collector concentration. Figure 4(a) reveals that the adsorption capacity of NaOl on the rutile surface is very high at pH of 8.5, which reaches the equilibrium value (approximately 13.15×10⁻⁶ mol/g) at the initial concentration of NaOl of 3.5×10⁻⁵ mol/L. SPA was barely adsorbed on the rutile surface at pH of 8.5. This is consistent with the

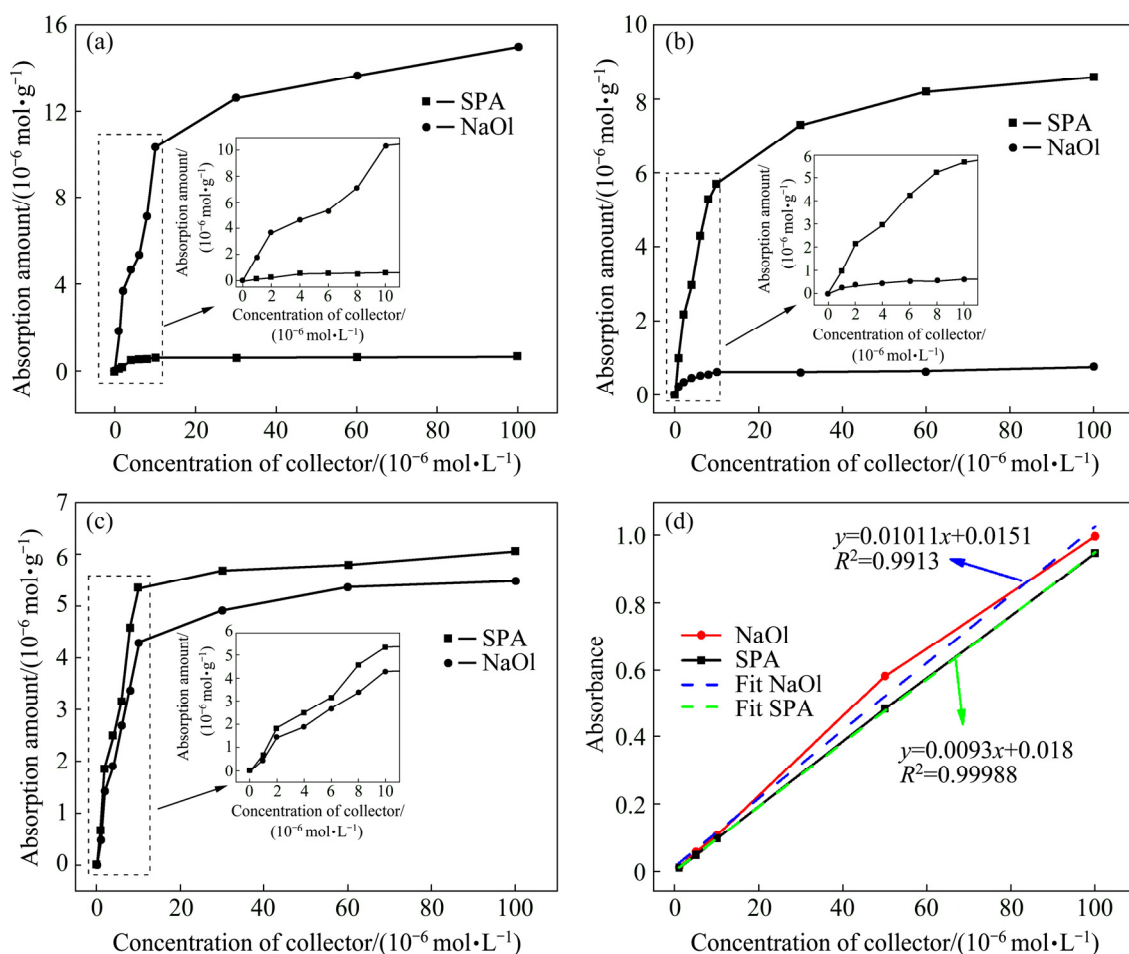


Fig. 4 Absorption amounts on rutile surface as function of collector concentration at pH of 8.5 (a) and 2.5 (b); Absorption treatment for 30 min at pH of 8.5, followed by pH adjustment to 2.5 (c) and absorbance calibration curves for NaOl and SPA (d)

flotation results of Figs. 2(b) and 3(b). Opposite results are observed in Fig. 4(b). SPA has a high adsorption capacity on the rutile surface at pH of 2.5, while NaOl has a low adsorption capacity. However, the adsorption equilibrium value (approximately 6.83×10^{-6} mol/g) of SPA at pH of 2.5 was lower than that of NaOl at pH of 8.5, which indirectly shows that the collection ability of NaOl was higher than that of SPA. The change in the pH value was inevitable in the conversion process of cleaning and roughing as shown in the flowsheet in Fig. 1(c). SPA and NaOl are adsorbed on the rutile surface for 30 min at pH of 8.5, followed by pH adjustment to 2.5. SPA and NaOl had high adsorption capacities on the rutile surface. Based on a comparison with Fig. 4(a), the adsorption equilibrium value (4.5×10^{-6} mol/g) of NaOl is reduced, compared with Fig. 4(b), its adsorption equilibrium value significantly increases. The adsorption equilibrium value of SPA in Fig. 4(c) is slightly smaller than that in Fig. 4(b). In Fig. 4(d), the analytical calibration curves are obtained by referencing standard solutions of 1, 5, 10, 50, and 100×10^{-6} mol/L of SPA, and NaOl. The R^2 of the fitting

curves were 0.9998 and 0.9913, which suggested that the standard curves were positively correlated with the study scope.

Figure 5 shows the adsorption amounts of SPA and NaOl on the amphibole surface as a function of the collector concentration. Figure 5(a) shows that the adsorption equilibrium value of NaOl is 7.3×10^{-6} mol/g; the adsorption reaches the equilibrium value at the NaOl initial concentration of 1.0×10^{-5} mol/L. Compared with Fig. 4(a), NaOl has a high adsorption capacity on the amphibole surface under weak alkaline conditions, leading to a low selectivity of NaOl. Figure 5(b) reveals that SPA and NaOl are not adsorbed on the amphibole surface at pH of 2.5. Figure 5(c) shows the results when SPA and NaOl are adsorbed on the amphibole surface for 30 min at a pH of 8.5, followed by pH adjustment to 2.5. The adsorptions of SPA and NaOl on the amphibole surface are small under this condition. Figures 4(c) and 5(c) reveal that the SPA and NaOl adsorptions on the rutile surface are large, while those on the amphibole surface are significantly smaller. This provides a theoretical basis for the flowsheet as shown in Fig. 1(c).

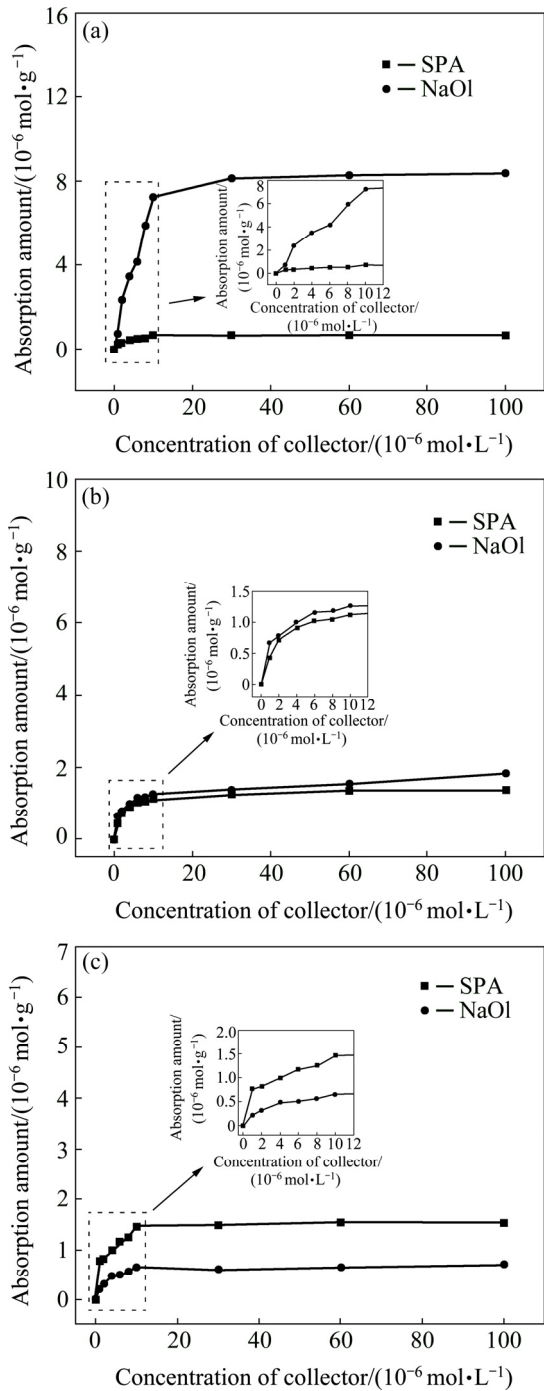


Fig. 5 Absorption amounts on amphibole surface as function of collector concentration at pH of 8.5 (a) and 2.5 (b), absorption treatment for 30 min at pH of 8.5, followed by pH adjustment to 2.5 (c)

3.4 Contact angle measurements

In order to illustrate the difference in hydrophobicity between the rutile and amphibole surfaces in the conversion process of cleaning and roughing in the flowsheet, shown in Fig. 1(c), we measure the contact angles on the rutile and amphibole surfaces. The results are shown in Fig. 6. Figure 6(a) shows that the contact angle of the rutile surface can

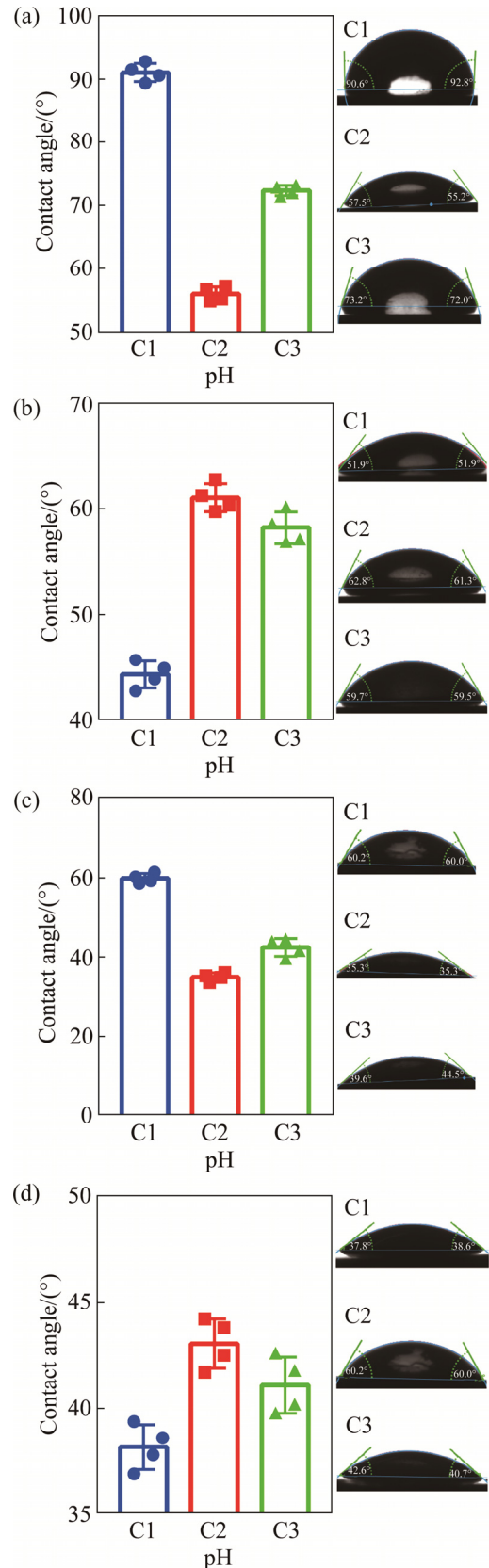


Fig. 6 Contact angles on mineral surfaces under different conditions: (a) NaOl and (b) SPA adsorbed on rutile surface, (c) NaOl and (d) SPA adsorbed on amphibole surface (C1: pH=8.5, C2: pH=2.5, C3: absorption treatment for 30 min at pH of 8.5, followed by pH adjustment to 2.5)

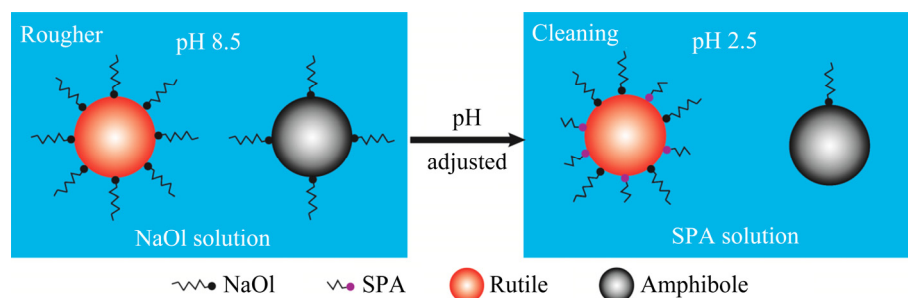


Fig. 7 Schematics of possible adsorption mechanisms of NaOI and SPA on rutile and amphibole surfaces

reach 91° after NaOI adsorption when pH is 8.5. However, when pH was 2.5, the contact angle was only 55.9° . When NaOI was adsorbed on the rutile surface for 30 min at pH of 8.5, followed by pH adjustment to 2.5, the contact angle could reach 72.0° . This suggested that after the pH adjustment, NaOI adsorbed on the rutile surface was transferred back to the solution; however, a significant fraction remained on the rutile surface. Figure 6(b) shows that the contact angle of the rutile surface is only 43.8° after SPA was adsorbed at pH of 8.5. However, at the final pH of 2.5, the contact angles reach 61.5° (C2) and 58.2° (C3). Figure 6(c) shows that the contact angle of the amphibole surface is 60.1° after NaOI adsorption when pH is 8.5. However, at the final pH value of 2.5, the contact angles of the amphibole surface decreased to 38.2° (C2) and 40.3° (C3). This indicates that when the pH was adjusted to 2.5, a significant amount of NaOI adsorbed at pH of 8.5 on the amphibole surface was transferred back to the solution. Figure 6(d) shows that the contact angles of the amphibole surface are very low for the three pH conditions. This shows that SPA hardly adsorbs on the amphibole surface.

4 Discussion

NaOI and SPA were utilized in the flotation separation of rutile and amphibole. Owing to the high collection ability and low cost, NaOI was used as a collector for roughing and scavenging, whereas SPA was used as the collector for cleaning owing to the high selectivity. Regarding the roughing and cleaning, we propose adsorption diagrams of NaOI and SPA on the rutile and amphibole surfaces, as shown in Fig. 7.

In the roughing, at conditions providing a high recovery rate, approximately 80% of the gangue minerals are discarded. After NaOI adsorption, there is a difference in hydrophobicity between the rutile and amphibole surfaces (Figs. 6(a) and (c)). However, the content of amphibole (67.33%) in the raw minerals was significantly higher than that of rutile (2.43%), which

suggests that amphibole still occupied a large proportion in the roughing production. In the cleaning, if NaOI was used as the collector under the same conditions, it was difficult to further separate rutile and amphibole. Therefore, we chose SPA as the collector for cleaning, which had a high selectivity but low collection ability.

In the cleaning, the pH of slurry was adjusted from 8.5 to 2.5, to improve the collection ability of SPA [8]. After the pH adjustment, NaOI, which was adsorbed to the rutile surface in the roughing, was only partially dissolved into the slurry. NaOI adsorbed on the amphibole surface was mostly dissolved. SPA was selectively adsorbed on the rutile surface, whereas it was hardly adsorbed on the amphibole surface at pH of 2.5, as shown by the adsorption amount and contact angle measurements. The rutile surface adsorbed not only a large amount of residual NaOI but also SPA. However, only a small amount of NaOI remained on the amphibole surface. Therefore, the hydrophobic difference between the rutile and amphibole surfaces was enhanced in the cleaning, and consequently their further separation became significantly easier.

5 Conclusions

(1) The reagent system of NaOI as a collector for roughing and scavenging and SPA as the collector for cleaning can effectively solve the problem of flotation separation of the primary rutile ore in Zaoyang mine in Hubei, China. The results showed that the grade of TiO_2 increased from 68.22% to 78.68%, while the recovery was reduced by only 2.5%. In addition, the dosage of SPA utilized in the new reagent system was only 20% of that of the old system, which enabled a significant cost reduction of reagents.

(2) After the pH of the solution changed from weakly alkaline to strong acidity, the rutile surface adsorbed not only a large amount of residual NaOI but also SPA; a small amount of NaOI remained on the amphibole surface.

References

- [1] TIMME S, TRAPPE V, KORZEN M, SCHARTEL B. Fire stability of carbon fiber reinforced polymer shells on the intermediate-scale [J]. *Composite Structures*, 2017, 178: 320–329.
- [2] WU B B, DING D H, PAN Z X, CUIURI D, LI H J, HAN J, FEI Z Y. Effects of heat accumulation on the arc characteristics and metal transfer behavior in wire arc additive manufacturing of Ti₆Al₄V [J]. *Journal of Materials Processing Technology*, 2017, 250: 304–312.
- [3] CHENG J, LI F, ZHU S Y, YU Y, QIAO Z H, YANG J. Electrochemical corrosion and tribological evaluation of TiAl alloy for marine application [J]. *Tribology International*, 2017, 115: 483–492.
- [4] NIE X, WEI X, LI X, LU C. Heat treatment and ventilation optimization in a deep mine [J]. *Advances in Civil Engineering*, 2018(4): 1–12.
- [5] ZAGHDOUDI M, FOURCADE F, SOUTREL I, FLONER D, AMRANE A, MAGHRAOUI-MEHERZI H, GENESTE F. Direct and indirect electrochemical reduction prior to a biological treatment for dimetridazole removal [J]. *Journal of Hazardous Materials*, 2017, 335: 10–17.
- [6] CHEN P, ZHAI J H, SUN W, HU Y H, YIN Z G, LAI X S. Adsorption mechanism of lead ions at ilmenite/water interface and its influence on ilmenite flotability [J]. *Journal of Industrial and Engineering Chemistry*, 2017, 53: 285–293.
- [7] CHEN P, ZHAI J H, SUN W, HU Y H, YIN Z G. The activation mechanism of lead ions in the flotation of ilmenite using sodium oleate as a collector [J]. *Minerals Engineering*, 2017, 111: 100–107.
- [8] XIAO W, CAO P, LIANG Q N, PENG H, ZHAO H B, QIN W Q, QIU G Z, WANG J. The activation mechanism of Bi³⁺ ions to rutile flotation in a strong acidic environment [J]. *Minerals*, 2017, 7(7): 113.
- [9] CHEN W, FENG Q, ZHANG G, YANG Q. Investigations on flotation separation of scheelite from calcite by using a novel depressant: sodium phytate [J]. *Minerals Engineering*, 2018, 126: 116–122.
- [10] PU X Z, CHEN F F, CHEN W, DING Y H. The effect of whey propein on the surface property of the copper-activated marmatite in xanthate flotation system [J]. *Applied Surface Science*, 2019, 479: 303–310.
- [11] CHACHULA, LIU Q. Upgrading a rutile concentrate produced from Athabasca oil sands tailings [J]. *Fuel*, 2003, 82(8): 929–942.
- [12] WANG J, CHENG H M, ZHAO H B, QIN W Q, QIU G Z. Flotation behavior and mechanism of rutile with nonyl hydroxamic acid [J]. *Rare Metals*, 2016, 35(5): 419–424.
- [13] LI H Q, MU S X, WENG X Q, ZHAO Y L, SONG S X. Rutile Flotation with Pb²⁺ Ions as Activator: Adsorption of Pb²⁺ at rutile/water interface [J]. *Colloids and Surfaces A: Physicochemical and Engineering Aspects*, 2016, 506: 431–437.
- [14] SINGH B, MERCIER-BION F, LEFEVRE G, SIMONI E. Effect of short chain aliphatic carboxylic acids for sorption of uranyl on rutile Zeta potential and in situ ATR-FTIR studies [J]. *Journal of Industrial & Engineering Chemistry*, 2016, 35: 325–331.
- [15] YU Y Y, GONG X Q. Unique adsorption behaviors of carboxylic acids at rutile TiO₂ (110) [J]. *Surface Science*, 2015, 641: 82–90.
- [16] BUCHHOLZ M, XU M, NOEI H, WEIDLER P, NEFEDOV A, FINK K, WANG Y M, WÖLL C. Interaction of carboxylic acids with rutile TiO₂ (110): IR-investigations of terephthalic and benzoic acid adsorbed on a single crystal substrate [J]. *Surface Science*, 2015, 643: 117–123.
- [17] MADELEY J, GRAHAM K. Flotation of rutile with anionic and cationic collectors [J]. *Journal of Applied Chemistry*, 1966, 16(6): 169–170.
- [18] LIU Q, PENG Y J. The development of a composite collector for the flotation of rutile [J]. *Minerals Engineering*, 1999, 12(12): 1419–1430.
- [19] XIAO W, KE S, QUAN N N, ZHOU L M, WANG J, ZHANG L J, DONG Y P, QIN W Q, QIU G Z, HU J. The role of nanobubbles in the precipitation and recovery of organic-phosphine-containing beneficiation wastewater [J]. *Langmuir*, 2018, 34(21): 6217–6224.
- [20] GAO Y S, GAO Z Y, SUN W, YIN Z G, WANG J J, HU Y H. Adsorption of a novel reagent scheme on scheelite and calcite causing an effective flotation separation [J]. *Journal of Colloid and Interface Science*, 2018, 512: 39–46.
- [21] XIAO W, FANG C J, WANG J, LIANG Q N, CAO P, WANG X X, ZHANG L J, QIU G Z, HU J. The role of EDTA on rutile flotation using Al³⁺ ions as an activator [J]. *RSC Advances*, 2018, 8(9): 4872–4880.
- [22] XIAO W, CAO P, LIANG Q N, HUANG X T, LI K Y, ZHANG Y S, QIN W Q, QIU G Z, WANG J. Adsorption behavior and mechanism of Bi(III) ions on rutile-water interface in the presence of nonyl hydroxamic acid [J]. *Transactions of Nonferrous Metals Society of China*, 2018, 28(2): 348–355.

油酸钠和苯乙烯膦酸在金红石和角闪石表面的吸附机制

肖巍^{1,2}, 任亚鑫¹, 杨娟¹, 曹攀², 王军², 覃文庆², 邱冠周²

1. 西安建筑科技大学 资源工程学院, 西安 710055; 2. 中南大学 资源加工与生物工程学院, 长沙 410083

摘要: 采用油酸钠和水杨羟膦酸作为枣阳原生金红石矿粗选和扫选的捕收剂, 苯乙烯膦酸和正辛醇作为精选的捕收剂的浮选药剂流程制度。浮选结果表明: 苯乙烯膦酸的用量减少 80%左右, 并且金红石精矿品位和回收率明显提高。吸附量和接触角测试揭示在酸性条件下金红石表面不仅吸附了大量残余的油酸钠, 同时还吸附了大量的苯乙烯膦酸, 然而角闪石表面仅吸附了微量的苯乙烯膦酸。捕收剂在矿物表面的这种吸附行为使得金红石和角闪石表面的疏水性差异被扩大, 它们的浮选分离也变得更加容易。

关键词: 金红石; 角闪石; 浮选分离; 组合捕收剂; 协同吸附机制